RSC Advances

ROYAL SOCIETY OF CHEMISTRY

www.rsc.org/advances

Synthesis and Evaluation of Stable Polymeric Solid Acid Based on Halloysite Nanotubes for Conversion of One-Pot Cellulose to 5-Hydroxymethylfurfural

Yunlei Zhang[a,b], Jianming Pan[a,b*], Yongsheng Yan[b], Weidong Shi[b*], Longbao Yu[b]

[a] School of the Environment and Safety Engineering, Jiangsu University, Zhenjiang 212013, China

[b] School of Chemistry and Chemical Engineering, Jiangsu University, Zhenjiang 212013, China

Abstract: Based on halloysite nanotubes (HNTs), precipitation polymerization and Pickering emulsion polymerization were firstly adopted to synthesize two composites i.e HNTs-polystyrene(PSt)-polydivinylbenzene(DVB)(I) and HNTs-PSt-PDVB(II), respectively. After sulfonation by 98% H_2SO_4, two polymeric solid acid catalysts i.e HNTs-PSt-PDVB-SO_3H(I) and HNTs-PSt-PDVB-SO_3H(II) were successfully prepared for conversion of one-pot cellulose to 5-hydroxymethylfurfural (HMF) in an ionic liquid 1-ethyl-3-methyl-imidazolium chloride ([EMIM]-Cl). Characterizations of two catalysts showed that HNTs-PSt-PDVB-SO_3H(I) possessed superiorer hydrophobicity, content of -SO_3H group, total acidic amounts than those of HNTs-PSt-PDVB-SO_3H(II), but with less very strong acidic sites and badly uniform morphology. Then the amount of the catalysts, reaction time and reaction temperature were optimized for cellulosic conversion over the two catalysts, and maximum yield of 28.52% for HNTs-PSt-PDVB-SO_3H(I) and 32.86% for HNTs-PSt-PDVB-SO_3H(II) at the optimized conditions were obtained, indicating very strong acidic sites palyed a key factor for cellulose conversion. In addition, as-prepared two catalysts could be very easily recycled at least five times without significant loss of catalytic activity.

Keywords: Halloysite Nanotubes (HNTs); Cellulose; Conversion; Precipitation Polymerization; Pickering Emulsion Polymerizations; 5-Hydroxymethylfurfural (HMF)

1. Introduction

As a key chemical platform for biofuels, the preparation of 5-hydroxymethylfurfural (HMF) from biomass is an important research topic. HMF, which has several different functional groups, can be converted to 2,5-dimethylfuran which is a biofuel just like gasoline and other important molecules such as levulinic acid, 2,5-furandicarboxylic acid, 2,5-diformylfuran, dihydroxymethylfuran and 5-hydroxy-4-keto-2-pentenoic acid.[1,2] So far, much efforts have been devoted to get HMF from biomass energy such as fructose, inulin and other fructose based carbohydrates.[3-5] Compared with other ones, the cellulose exist abundantly in the nature world and easily got attracted much attention.[6-8] However, cellulose cannot be dissolved in traditional solvents such as H_2O, ethyl acetate, acetonitrile, aether.[9,10] Recently, ionic liquids i.e ILs (such as 1-butyl-3-methylimidazolium chloride ([BMIM]-Cl), 1-ethyl-3-methyl-imidazolium chloride ([EMIM]-Cl), 1-carboxyethyl-3-methylimidazolium chloride ([C_1COOHmim]-Cl), 1-butyl-3-methylimidazolium hydrogensulfate ([Bmim]HSO_4) and so on) and some bifunctional ionic liquids have been appeared to solve this problem.[1,11]

Up till now, the mechanism of cellulose conversion could be considered to have three main reactions: (1) cellulose-to-glucose depolymerization, (2) glucose-to-fructose isomerization, and (3) fructose-to-HMF dehydration.[12] It is believed that acid catalysts are helpful for accelerating the hydrolysis of cellulose.[13] Furthermore, previous studies have shown that the morphology of solid catalysts greatly affects their catalytic performance because of the influence of morphology on the diffusion length of the reactants and products, the exposure degree of active sites, and so on. So, catalysts with well defined morphology is also essential, therefore high accessibility of the active sites and fast diffusion of the reactants and the products can be guaranteed.[14] So far, the acid catalysts used to degrade the biomass can be classified as conventional mineral acids (such as H_2SO_4 and HCL),[15-18] lewis acids and organic polymer acids. Julien et al. treated the cellulose at the vacuum pyrolysis of acid-impregnated (H_2SO_4, HCl, HNO_3).[19] Hussein's group used $CrCl_3$ and $CrCl_3$/$CuCl_2$ catalysts in 1-ethyl-3-methylimidazolium chloride ([EMIM]-Cl) ionic liquid to degrade the cellulose directly to the HMF, and got well yield of HMF.[20] However, homogeneous superacids are usually highly toxic, environmentally hazardous, and cannot be easily recovered from the products mixture, which largely constrain their wide applications in industry.[21] Recently, organic solid polymer catalysts with well defined morphology have attracted much attention

because the shortened diffusion lengths can not only increase the reaction rates, but also can improve selectivity by decreasing the possibility for side reactions, especially for the deep reactions of the unstable products.[22,23] Among various acid catalysts, the organic polymer acids showed very important applications because of their heterogeneous catalytic performance when compared with conventional mineral acids and lewis acids. Additionally, the unique strong acid strength results in their extra-ordinary catalytic activities in cellulose degradation. In Liu's work, they firstly synthesized the superhydrophobic mesoporous polydivinylbenzene (PDVB) by polymerization of divinyl benzene (DVB) under solvothermal condition, and then took the PDVB as carrier and sulfonated by chlorosulfonic acid and CH_2Cl_2 to form PDVB-SO_3H.[15] Li's group coupled the 1-vinyl-3-propane sulfonate imidazolium (VMPS) and azobisisobutyronitrile (AIBN) together to polymerize the PVMPS as carrier for further functionalized with monomers of -SO_3H and Cr(III) to get functional polymeric ionic liquids (FPILs).[24] Good results have been achieved for catalysts preparing in using above methods and also got well yield of HMF toward cellulose conversion. Nevertheless, the mechanical properties of catalysts mentioned above are not very well and the catalysts preparation process are relatively more complex and time consuming. Therefore, looking for the new ways of preparing organic polymer acids are still needed the further study and also having the significant meaning in solving some problems in the catalytic field.

Precipitation polymerization, one of the polymerization approaches, which are mostly heterogeneous polymerization systems, has received particular attention because of its easy operation and no need for any surfactant or stabilizer.[25-27] Chen et al. firstly used the method of precipitation polymerization for preparing microspheres, which expected to find practical applications as novel heat-resistant additives, solid carriers for catalysts, and so on.[28] The emulsions stabilized by solid particles instead of emulsifier, so-called Pickering emulsion is another excellent way to get organic polymer composites. Compared with traditional emulsion polymerization methods, the solid particles used in the Pickering emulsion adsorbed at the oil-water interface act as the effective stabilizers during the polymerization process with no need for any conventional stabilizers when Pickering emulsion droplets are used as polymerization vessels.[29] Jiang's group firstly got biocatalyst for biodiesel production through Pickering emulsion stabilized by lipase-containing periodic mesoporous organosilica (PMO) and the Pickering

emulsion showed outstanding activity, mechanical and storage stability.[30] Various solid particles appeared in this field used for preparing the Pickering emulsion, such as polystyrene/clay,[31] poly(vinyl acetate)/SiO_2[32] and so on. Furthermore, several reports adopted spherical particles to irreversibly adsorb at oil and water interface, whereas for non-spherical shape colloids at free interfaces capillary interaction appear to be dominant in Pickering emulsion stabilizers.[33,34] So, looking for a new kind of non-spherical particles as Pickering emulsion stabilizers showed the vital significance.

Recently, the natural clay-particles, widely distributed around the world of rock and soil have been used in many studies such as the clay-based heterogeneous catalysts in green catalysis.[35] Typically, halloysite nanotubes (HNTs) is an aluminosilicate clay mined from natural deposits and having a hollow microtubular and non-spherical structure rather than a stacked plate-like structure,[36] which will be favorable to the diffusion of polymers grafted onto not only HNT tubes, but also easier onto halloysite sheets. What's more, HNTs has high surface area and a few hydroxyl groups,[37] indicating that some larger molecules are easier to be adsorbed onto its surface. Thanks to the excellent properties, HNTs are the prefect supporter of the precipitation polymerization and stabilizer of the Pickering emulsion. Best to our knowledge, there were no reports of using the HNTs by precipitation polymerization and Pickering emulsion polymerizations for preparing polymeric solid acids in the catalytic field. What's more, in our previous work, we have already found that HNTs with functional groups is efficient solid catalysts supporter for conversion of one-pot cellulose to HMF.[38] However, the use of HNTs as catalysts supporter is still in its infancy.

Enlightened by the information mentioned above, we reported here two methods of making organic polymer acids for conversion of one-pot cellulose to HMF in ILs of [EMIM]-Cl. The first sample was made by precipitation polymerization using HNTs as supporter, while the another sample was produced by Pickering emulsion polymerizations taking the HNTs as the stabilizer. After sulfonated by 98% H_2SO_4 to introduce the group of -SO_3H, two polymeric solid acidic catalysts denoted as HNTs-PSt-PDVB-SO_3H(I) and HNTs-PSt-PDVB-SO_3H(II) were obtained. The morphology and various properties of the two samples were characterized and the reaction time, temperature and catalysts loading amounts in order to find the optimized conditions in the

system containing catalysts of HNTs-PSt-PDVB-SO_3H(I) and HNTs-PSt-PDVB-SO_3H(II) were discussed in detail. Moreover, this two catalysts showed good recyclability and thermostability.

2. Experimental section

2.1. Chemicals and reagents

HNTs was collected from Zhengzhou Jinyangguang Chinaware Co. Ltd., Henan, China. Prior to use, HNTs was refluxed by a certain concentration of HNO_3. In a typical run, 40 g of HNTs were dealed with 250 mL 3.0 M HNO_3 at 75 ^oC for 12 h, and then cooled to room temperature. After the filtration to achieve the pH to 7.0, the obtained powders were calcined at 200 ^oC for 2.0 h. The resulting nanocomposites were denoted as treated HNTs. 1-ethyl-3-methyl-imidazolium chloride ([EMIM]-Cl), cellulose (powder, ca. 50 micron), 5-HMF (>99%), trimethylolpropane trimethacrylate (TRIM), 3-(trimethoxysilyl) propylmethacrylate (TMSPMA, 98%), 2,2′-Azobis (2-methyl-propionitrile) (AIBN, 99%), and Divinylbenzene (DVB) were obtained from Aladdin Reagent Co., Ltd. (Shanghai, China) and used as received. NaCL, styrene (St), methanol, ethanol, dry toluene, dimethyl 2,2'-azobis(2-methylpropionate) and HPLC-grade methanol were purchased from Sinopharm Chemical Reagent Co., Ltd. (Shanghai, China). H_2SO_4 (98%) and HNO_3 were obtained from Yangzhou-Shanghai Bao Chemical Co., Ltd. (Shanghai). All other chemicals were supplied by local suppliers and used without further purification.

2.2 Preparation of vinyl-modified HNTs

2.0 g of treated HNTs were dispersed into 100 mL of dry toluene by ultrasonic vibration, and then 4.0 mL of TMSPMA was slowly injected into the mixture under nitrogen at 90 ^oC, and the reaction were then proceeded for 24 h under the mechanical stirring. After cooling, the resulting products were collected and washed with fresh toluene for several times, and then dried in vacuum at 60 ^oC overnight. The final products were named as vinyl-modified (V-HNTs).

2.3 Synthesis of HNTs-PSt-PDVB(I) by precipitation polymerization

Synthesis of HNTs-PSt-PDVB(I) by precipitation polymerizations was implemented by following steps mentioned in the previous literature with a slight modification,[39] where St was adopted as the functional monomer, TRIM and DVB as the cross-linker and the AIBN as the initiator, respectively. As a typical run of preparing HNTs-PSt-PDVB(I), 0.5 g of V-HNTs was added to 250 mL three-necked flask, and then the dispersing solution St (79.6 mmol), cross-linker (TRIM, 8.0 mmol and DVB, 8.0 mmol), initiator (AIBN, 0.6 mmol), and dispersing medium (water, 80 mL) were adequately mixed and dispersed by vigorous agitation (600 rpm), bubbled with a nitrogen stream throughout the procedure. The polymerization was completed at 70°C for 24 h. The

resulting HNTs-PSt-PDVB(I) were separated from the mixed solution with the help of filtration, and were then washed with toluene and methanol several times. Finally, the products HNTs-PSt-PDVB(I) were dried in vacuum at 60 ^{o}C overnight to get powders.

2.4 Synthesis of HNTs-PSt-PDVB(II) by Pickering emulsion polymerization

HNTs-PSt-PDVB(II) was synthesized by Pickering emulsion polymerization. A typical procedure was detailed as follows: aqueous phase were formed by adding 0.572 g of NaCL, 0.3 g of treated HNTs to 25 mL of water, and oil phase were contained toluene (0.14 mL), St (2.0 mL) and DVB (2.0 mL). Followed by emulsification of the mixture of aqueous phase and oil-phase by an ultrasonic processor for 10 min and under nitrogen stream for 20 min to form a stable o/w Pickering emulsion. The obtained emulsion was subsequently polymerized at 65 ^{o}C in the presence of 0.12 mL of dimethyl 2,2'-azobis(2-methylpropionate) for 12 h. The obtained composites HNTs-PSt-PDVB(II) were filtrated and washed with toluene and methanol respectively, followed by being dried in vacuum at 25 ^{o}C.

2.5 Sulfonation of as-prepared HNTs-PSt-PDVB(I) and HNTs-PSt-PDVB(II)

To obtain the solid acid catalysts, the as-prepared HNTs-PSt-PDVB(I) and HNTs-PSt-PDVB(II) were sulfonated by 98% H_2SO_4. In a typically run, HNTs-PSt-PDVB(I) was added to the 98% H_2SO_4 at the ratio of 30 mL per gram. To ensure homogeneous dispersion of HNTs-PSt-PDVB(I), the reaction was carried out in a oil bath oscillator with a rate of 800 rpm under 70 ^{o}C. Same procedure was taken out for the sulfonation of as-prepared HNTs-PSt-PDVB(II). To the end, the products were filtrated and washed with water and dried at 60 ^{o}C, respectively. The ultima catalysts named as HNTs-PSt-PDVB-SO_3H(I) and HNTs-PSt-PDVB-SO_3H(II), respectively.

2.6. Characterization of HNTs-PSt-PDVB-SO_3H(I) and HNTs-PSt-PDVB-SO_3H(II)

The morphology of HNTs-PSt-PDVB-SO_3H(I) and HNTs-PSt-PDVB-SO_3H(II) were observed by scanning electron microscope (SEM, S-4800). TGA of samples were performed for powder samples (about 10 mg) using a Diamond TG/DTA instruments (Perkin–Elmer, U.S.A) under a nitrogen atmosphere up to 800 ^{o}C with a heating rate of 5.0 ^{o}C/min. XPS spectra were performed on a Thermo ESCALAB 250 with Al Kα radition at y = 901 for the X-ray sources, the binding energies were calibrated using the C_{1s} peak at 284.9 eV. The acidic features including the strength of the acid center from 30 ^{o}C to 700 ^{o}C of HNTs-PSt-PDVB-SO_3H(I) and HNTs-PSt-PDVB-SO_3H(II) solid acid catalysts were determined by means of temperature

programmed desorption (NH_3-TPD) using a TP 5000-II multiple adsorption apparatus (Tianjin Xianquan Corporation of Scientific Instruments, China) in which taking chromatographic thermal conductivity detector, NH_3 as the adsorbate, He as the carrier gas. FTIR spectra were obtained using the KBr pressed pellet method with a Bruker VERTEX 70 Fourier transform infrared spectrometer. The KBr pellets were prepared by pressing mixtures of catalysts to KBr at the mass ratio of 1:100. All spectra were collected at room temperature using 64 scans in the range of 4000-400 cm^{-1} with a resolution of 4 cm^{-1}. The morphology of the synthesized by Pickering emulsion polymerization dried particles was observed by a type of BM-59XCC optical microscope (BMCO., LTD, China).

2.7. Catalytic reactions

2.7.1 Typical procedures for cellulose hydrolysis using HNTs-PSt-PDVB-SO_3H(I) and HNTs-PSt-PDVB-SO_3H(II) as catalysts in ionic liquids

Experiments were carried out in 25 mL graduated pyrex glass tube immersed in an oil bath preheated at the required temperature using a hot plat with a digital magnetic stirrer. The cellulosic conversion included two steps of pre-treatment and reaction. In a typical experiment for pre-treatment, cellulose (0.1 g) was added into 2.0 g of [EMIM]-Cl, and the whole mixture was heated at 120 ^oC and stirred at 800 r min^{-1} for 0.5 h for dissolution of cellulose. For the typical reaction step, catalyst (0.1 g) was added into the cellulose/[EMIM]-Cl solution while keeping heating and stirred at 800 r min^{-1} at the optimized conditions. All reaction steps were repeated three times.

Cellulose conversion was obtained by the change of cellulose weight before and after the reaction. The yield of products were calculated from the equation:

$$\text{yield}(\%) = \frac{\text{weight of products}}{\text{weight of cellulose put into the reactor}} \times 100\%$$

2.7.2 HMF testing

The HMF was analyzed by 1200 Agilent High Performance Liquid Chromatography (HPLC) equipped with Agilent TC-C18(2) Column (4.6×250 mm,5.0 μm) and Uv detector. During this process, the column temperature remain constantly at 25 ^oC, and the mobile phase was methanol-water (7:3, v/v) at flow rate of 0.7 mL min^{-1} with Uv detection at 283 nm, and 22.5 μL of each sample was also injected manually. The concentration of HMF was calculated based on

the standard curve obtained with standard substances. Standard curve was showed below. Within the scope of the experiment, the concentration had good linear relationship with the peak area.

Insert Fig.1 Calibration curve of HMF

3. Results and discussion

3.1. Structural characterizations of catalysts

The morphology of the synthesized materials were characterized with SEM and optical microscope. As shown in Fig. 2a and Fig. 2b, both HNTs-PSt-PDVB(I) and HNTs-PSt-PDVB(II) exhibited spherical structure with the diameter from 27~60 μm for HNTs-PSt-PDVB(I), while the HNTs-PSt-PDVB(II) has the relatively uniform average diameter of about 13μm. Interestingly, when compared with Fig. 2c and Fig. 2e, which representing the magnified images of the surface of HNTs-PSt-PDVB(I) and HNTs-PSt-PDVB(II), respectively. It can be clearly seen that the great majority of the surface for HNTs-PSt-PDVB(I) was coated with spherical and hydrophobic polymer, while lots of tubular morphology of hydrophilic HNTs appeared in Fig. 2e for HNTs-PSt-PDVB(II). Fig. 2d and Fig. 2f represented the morphology of final catalysts of HNTs-PSt-PDVB-SO_3H(I) and HNTs-PSt-PDVB-SO_3H(II), respectively. According to the results in the Fig. 2d and Fig. 2f, it could be found that the sulfonation process does not damage the structure and morphology of HNTs-PSt-PDVB(I) and HNTs-PSt-PDVB(II). Compared with the method of precipitation polymerization, the Pickering emulsion polymerizations for polymerization can obtain a more uniform distribution of morphology. As seen in Fig. 2g, droplets of Pickering emulsion solely stabilized by HNTs revealed to be polydisperse, indicating the solid particle-adsorbed interfaces provided enough stability against droplet. Moreover, by heating at 65 ^{o}C to initiate polymerizations, as-prepared HNTs-PSt-PDVB microspheres were coarse and symmetrical without slight dimple. Fig. 2h showed the optical micrograph of final dried solid catalyst, and it can be seen that the spherical structure maintained well when particles dried to get solid catalyst.

Insert Fig. 2 (A) SEM of the HNTs-PSt-PDVB(I) (a、c), HNTs-PSt-PDVB(II) (b、e) and HNTs-PSt-PDVB-SO_3H(I) (d), HNTs-PSt-PDVB-SO_3H(II) (f). (B) Optical micrographs of Pickering emulsion polymerizations (g) and final dried solid catalyst of HNTs-PSt-PDVB-SO_3H(II) (h).

EDS analysis equipped with SEM for HNTs-PSt-PDVB(I), HNTs-PSt-PDVB-SO_3H(I) and HNTs-PSt-PDVB(II), HNTs-PSt-PDVB-SO_3H(II) were listed in Fig. 3a, Fig. 3b and Fig. 3c, Fig. 3d, respectively. When compared with Fig. 3a and Fig. 3b, we can see that a new peak of element S emerged in Fig. 3b. Same phenomenon was also appeared when compared with Fig. 3c and Fig. 3d. Interestingly, from the pictures of Fig. 3b and Fig. 3d, it can be observed that the more sharp peaks of the elements of S and O, probably due to be more adequately sulfonated in the sulfonation process for HNTs-PSt-PDVB(I). Same as the SEM observation, the arising peak of elements Al, Si indicated the raw material of HNTs used as catalysts supporter. Additionally, the results of element analysis for HNTs-PSt-PDVB(I), HNTs-PSt-PDVB-SO_3H(I) and HNTs-PSt-PDVB(II), HNTs-PSt-PDVB-SO_3H(II) were also shown in the corresponding figures. Same with the EDS analysis, the weight of S were both increased in the HNTs-PSt-PDVB-SO_3H(I) and HNTs-PSt-PDVB-SO_3H(II) when compared with HNTs-PSt-PDVB(I) and HNTs-PSt-PDVB(II), while the elements of C and H, especially the C, were both reduced during the sulfonation process. More spherical and hydrophobic polymers surrounded on the surface of HNTs-PSt-PDVB(I) than that of HNTs-PSt-PDVB(II) (when compared with Fig. 2c and Fig. 2e) were benefit for sulfonating process, which led to the corresponding results shown in EDS and element analysis.

Insert Fig. 3 Energy Dispersive Spectrometer (EDS) and element analysis of the HNTs-PSt-PDVB(I) (a), HNTs-PSt-PDVB-SO_3H(I) (b) and HNTs-PSt-PDVB(II) (c), HNTs-PSt-PDVB-SO_3H(II) (d).

Fig. 4 showed the contact angle of HNTs-PSt-PDVB(I) (Fig. 4a), HNTs-PSt-PDVB-SO_3H(I) (Fig. 4b) and HNTs-PSt-PDVB(II) (Fig. 4c), HNTs-PSt-PDVB-SO_3H(II) (Fig. 4d) for water. Clearly, HNTs-PSt-PDVB(I) exhibited the contact angle for the water up to 107.14^o, indicating its excellent hydrophobicity. On the contrary, for the HNTs-PSt-PDVB(II), it obtained the contact angle at 86.69^o, indicating its very relatively hydrophilic. The superior hydrophobic active site in HNTs-PSt-PDVB(I) also proved that much more hydrophobic polymer surrounded on its surface, while more hydrophilic HNTs encompassed on the surface of HNTs-PSt-PDVB(II). When compared with Fig. 4a and Fig. 4b, the contact angle was reduced from 107.14^o to 101.29^o, indicating the hydrophilic group -SO_3H was introduced onto the HNTs-PSt-PDVB(I), and the Same conclusion can also be drawn when compared with Fig. 4c and Fig. 4d.

Insert Fig. 4 Contact angle for water of HNTs-PSt-PDVB(I) (a), HNTs-PSt-PDVB-SO_3H(I) (b) and HNTs-PSt-PDVB(II) (c), HNTs-PSt-PDVB-SO_3H(II) (d).

3.2 Active site characterizations

Fig. 5a and 5b showed the X-ray photoelectron spectroscopy (XPS) measurements of HNTs-PSt-PDVB-SO_3H(I) and HNTs-PSt-PDVB-SO_3H(II), respectively. And the Fig. 5c, Fig. 5d, Fig. 5e and Fig. 5f, Fig. 5g, Fig. 5h described the magnified signals of $S_{2p,}$ O_{1s} and C_{1s} respectively. Clearly, both the HNTs-PSt-PDVB-SO_3H(I) and HNTs-PSt-PDVB-SO_3H(II) exhibited the signals of Al and Si, indicating the presence of HNTs in the HNTs-PSt-PDVB-SO_3H(I) and HNTs-PSt-PDVB-SO_3H(II), respectively. Interestingly, two new signals of O_{1s} and C_{1s} around at 284 eV and 532 eV can also be observed in HNTs-PSt-PDVB-SO_3H(I), confirming successfully polymerizing the macromolecule of PSt and PDVB onto the raw HNTs particles. The same phenomenon was also obtained when making the study of HNTs-PSt-PDVB-SO_3H(II). Except for C, O, Al and Si, a new signal at around 168 eV for HNTs-PSt-PDVB-SO_3H(I) and 154 eV, 168 eV for HNTs-PSt-PDVB(II) associated with S_{2p} and S_{2s} can also be observed in HNTs-PSt-PDVB-SO_3H(I) and HNTs-PSt-PDVB-SO_3H(II) confirming successfully grafting of -SO_3H onto the network of HNTs-PSt-PDVB(I) and HNTs-PSt-PDVB(II), respectively, which plays a key factor for increasing the acid strength of HNTs-PSt-PDVB-SO_3H(I) and HNTs-PSt-PDVB-SO_3H(II). This acid strength provide the abundant acidic sites, and the acidic sites can enhance the catalytic performance for the conversion of cellulose to HMF.[21] Thus, the organic polymer acids supported by natural clay may be the effective catalysts for the degradation of cellulose to HMF.

Insert Fig. 5 X-ray photoelectron spectroscopy (XPS) of the HNTs-PSt-PDVB-SO_3H(I) (a) and HNTs-PSt-PDVB-SO_3H(II) (b).

Fig. 6 revealed the FT-IR spectra of HNTs-PSt-PDVB(I) (Fig. 6a), HNTs-PSt-PDVB-SO_3H(I) (Fig. 6b) and HNTs-PSt-PDVB(II) (Fig. 6c), HNTs-PSt-PDVB-SO_3H(II) (Fig. 6d). The FTIR spectrum of this four samples all showed that bands in the region around at 3000 cm^{-1} assigned to the C-H stretching vibration of hydrocarbons were absent, indicating the existence of benzene ring in these samples.[40] Furthermore, the band at 1720 cm^{-1} that corresponded to the carbonyl groups confirmed that vinyl groups were successfully introduced to the surface of the treated HNTs by the

silanization reaction.[41] Compared with HNTs-PSt-PDVB(I), the peak around 670 cm^{-1} and 829 cm^{-1} associated with C-S bond can be clearly found in the sample of HNTs-PSt-PDVB-SO_3H(I), indicating the introduce of sulfonic group in this sample.[42] It can also clearly see that the peak around at 1105 cm^{-1} associated with C-S indicating the presence of sulfonic group for HNTs-PSt-PDVB-SO_3H(II).[43,44] The results confirmed that the organic polymer composites and sulfonic group were successfully obtained, which were in good agreement with XPS analysis results.

Insert Fig. 6 FT-IR spectra of HNTs-PSt-PDVB(I) (a), HNTs-PSt-PDVB-SO_3H(I) (b) and HNTs-PSt-PDVB(II) (c), HNTs-PSt-PDVB-SO_3H(II) (d).

3.3. Acidic features of HNTs-PSt-PDVB-SO_3H(I) and HNTs-PSt-PDVB-SO_3H(II)

The acidic features of obtained organic polymer acidic catalysts were determined by means of temperature programmed desorption (NH_3-TPD). The NH_3-TPD curves of HNTs-PSt-PDVB-SO_3H(I) and HNTs-PSt-PDVB-SO_3H(II) were shown in Fig. 7a and Fig. 7b, respectively. Among the desorbed NH_3 molecules, those appearing at ≤150 ^oC should correspond to the physically adsorbed and hydrogen-bound NH_3,[45] and other desorbed NH_3 molecules at the higher temperatures were attributed to acid site-bound NH_3.[46] The acid sites could be defined as weak, medium, strong and very strong at desorption temperatures of 150 ^oC-250 ^oC, 250 ^oC-350 ^oC, 350 ^oC-500 ^oC, and >500 ^oC, respectively.[47] It can be clearly seen that medium, strong and very strong acid sites existed in HNTs-PSt-PDVB-SO_3H(I) centered at 250 ^oC, 420 ^oC and 560 ^oC, indicating the presence of relatively moderate strong acidic sites and very strong acidic sites, respectively. Compared with the HNTs-PSt-PDVB-SO_3H(I), HNTs-PSt-PDVB-SO_3H(II) also emerged three peaks around 250 ^oC, 350 ^oC, and 530 ^oC, which could be assigned to the moderate strong acidic sites and strong acidic sites. The total acid amounts of HNTs-PSt-PDVB-SO_3H(I) and HNTs-PSt-PDVB-SO_3H(II) could be expressed by the amount of NH_3 bound to the acid sites, which was obtained by the total NH_3 amount subtracting that of physically adsorbed and hydrogen-bound NH_3. In contrast to HNTs-PSt-PDVB-SO_3H(II), which has a total acidic amounts of 237 μmol g^{-1} and separated acidic amounts of 16 μmol g^{-1}, 36 μmol g^{-1}, and 185 μmol g^{-1} for the acidic strengths of 250 ^oC, 350 ^oC and 530 ^oC, while HNTs-PSt-PDVB-SO_3H(I) has the total

acidic amount of 312 μmol g^{-1} and exhibited separated acidic amounts of 72 μmol g^{-1}, 152 μmol g^{-1}, and 88 μmol g^{-1} for various acidic strengths of 250 ^{o}C, 420 ^{o}C and 560 ^{o}C, respectively. As a result, HNTs-PSt-PDVB-SO_3H(I) possessed much stronger acid strength and more strong acidic sites. The existence of the strong acidic feature i.e. 420 ^{o}C, 560 ^{o}C for HNTs-PSt-PDVB-SO_3H(I) and 350 ^{o}C, 530 ^{o}C for HNTs-PSt-PDVB-SO_3H(II) in catalysts could be significant for efficient cellulose conversion.

Insert Fig. 7 Temperature programmed desorption (NH_3-TPD) of the HNTs-PSt-PDVB-SO_3H(I) (a) and HNTs-PSt-PDVB-SO_3H(II) (b).

3.4. Thermal stability

TG analysis was employed to estimate the weight ratio of inorganic and organic components, as shown in Fig. 8a for HNTs-PSt-PDVB-SO_3H(I) and Fig. 8b for HNTs-PSt-PDVB-SO_3H(II), respectively. Interestingly, HNTs-PSt-PDVB-SO_3H(II) showed obvious weight loss at 25-200 ^{o}C, assigned to the desorption of water. In contrast, HNTs-PSt-PDVB-SO_3H(I) showed a lower weight loss than HNTs-PSt-PDVB-SO_3H(II). This phenomenon indicated the lower adsorption content of water on HNTs-PSt-PDVB-SO_3H(I), which might be due to the excellent hydrophobicity of HNTs-PSt-PDVB-SO_3H(I). With increasing the temperature, HNTs-PSt-PDVB-SO_3H(I) and HNTs-PSt-PDVB-SO_3H(II) exhibited obvious weight loss attributed to the decomposition of sulfonic groups and network between 200 ^{o}C-800 ^{o}C, respectively.[48] Notably, the weight loss of the organic components between 200 ^{o}C-800 ^{o}C were 81.18% for HNTs-PSt-PDVB-SO_3H(I) and 33.44% for HNTs-PSt-PDVB-SO_3H(II). These results suggested that HNTs-PSt-PDVB-SO_3H(II) has superior thermal stability than HNTs-PSt-PDVB-SO_3H(I).[49]

Insert Fig. 8 TG curves of (a) HNTs-PSt-PDVB-SO_3H(I) and (b) HNTs-PSt-PDVB-SO_3H(II).

3.5. Catalytic activities

To obtain the optimum conditions for cellulose hydrolysis, ILs and a catalytic amount of catalysts were used as to investigate the influence of different factors. Variables for the hydrolytic process, such as reaction temperature, reaction time, catalyst dosage were studied in the reactors. Here, we adopted our optimized reaction conditions as: t_{dis} (dissolution time) = 0.5 h, T_{dis} (dissolution temperature) =120 ^{o}C, t_{rxn} (reaction time) =1.0 h, T_{rxn} (reaction temperature) =110 ^{o}C for the

catalyst of HNTs-PSt-PDVB-SO_3H(I) based system and t_{dis} (dissolution time) = 0.5 h, T_{dis} (dissolution temperature) =120 ^oC, t_{rxn} (reaction time) =2.0 h, T_{rxn} (reaction temperature) =120 ^oC for the system contained catalyst of HNTs-PSt-PDVB-SO_3H(II), respectively.

3.5.1 Effect of reaction temperature and time

As shown in Fig. 9a and Fig. 9b represented for HNTs-PSt-PDVB-SO_3H(I) and HNTs-PSt-PDVB-SO_3H(II), respectively. Temperature ranged from 100 ^oC to 140 ^oC were discussed at different time of 1.0 h, 2.0 h, 3.0 h, 4.0 h and same amount of 0.1g both for HNTs-PSt-PDVB-SO_3H(I) and HNTs-PSt-PDVB-SO_3H(II). When the temperature significantly increased, because of some side reactions such as formation of insoluble humines and soluble polymers (kinds of decomposition product of fructose) that preferred to occur when the temperature was closed to the melting point of monosaccharides.[50] What's more, increasing the reaction temperature can result in decomposition of HMF to other byproducts. Some possible byproducts such as formic acid and levulinic acid were examined by us, but could not be detected. Several work have also reported the decomposition of HMF to some unidentified products.[50,51]

It has reported that hydrophobic catalyst has great influence on the product of HMF stabilization.[52,53] When prolong the reaction time, it becomes an energetically spontaneous process in terms of water moving close to the HMF molecule. When prolonged optimized reaction time, catalysts with not superhydrophobic property may cause the the major side-reaction produced by acid-catalyzed hydration of HMF to levulinic acid (LA) and formic acid (FA)[54], and the HMF yield synchronously reduced. Thus the appropriate reaction temperature and reaction time were 1.0 h, 110 ^oC for HNTs-PSt-PDVB-SO_3H(I) and 2.0 h, 120 ^oC for HNTs-PSt-PDVB-SO_3H(II), respectively. And 28.52% yield of HMF obtained at the optimized conditions of HNTs-PSt-PDVB-SO_3H(I), while 24.28% yield of HMF for HNTs-PSt-PDVB-SO_3H(II), which systems all contained 0.1 g of catalysts.

Insert Fig. 9 (A) Effect of time and temperature on the yield of cellulose to HMF for HNTs-PSt-PDVB-SO_3H(I) (a) and HNTs-PSt-PDVB-SO_3H(II) (b). (B) Effect of catalyst amount (c).

3.5.2 Effect of catalysts loading amount

Fig. 9c shows the effect of the different catalysts dosages ranged from 0.05 g to 0.15 g on the HMF yield from cellulose at the optimized conditions for HNTs-PSt-PDVB-SO_3H(I) and HNTs-PSt-PDVB-SO_3H(II), respectively. According to various reports, acid catalysts were active in the direct hydrolysis of cellulose to glucose, HMF and other soluble by-products.[55-57] However, over-used catalysts led to side reaction in the dehydration of byproducts also accelerates. Results revealed that 0.1 g for HNTs-PSt-PDVB-SO_3H(I) and 0.05 g for HNTs-PSt-PDVB-SO_3H(II) at the optimized conditions can achieve the highest yield of HMF at 28.52% and 32.86%, respectively. Table 1 showed acid strength, contact angle and highest yield of HMF for the two catalysts. It could be observed that higher total acid strength for HNTs-PSt-PDVB-SO_3H(I) (312 μmol g^{-1}) than HNTs-PSt-PDVB-SO_3H(II) (237μmol g^{-1}), but less acid strength for very strong acidic sites of HNTs-PSt-PDVB-SO_3H(I) (88 μmol g^{-1}) comparatively speaking of HNTs-PSt-PDVB-SO_3H(II) (185 μmol g^{-1}). Thus, the low yield of HMF by HNTs-PSt-PDVB-SO_3H(I) suggested that existing of acid strength for very strong acidic sites played a key factor for cellulose conversion. Even though the HNTs-PSt-PDVB-SO_3H(I) show more hydrophobic (101.29^o) than that of HNTs-PSt-PDVB-SO_3H(II) (85.14^o), its particle size possessed badly uniform distribution. It could be concluded that the morphology of solid catalysts also greatly affected their catalytic performance.

Insert Table. 1 Acid strength and highest yield of HMF for the two catalysts

3.6. Recyclability of the catalysts

To make a further study the recyclability of the synthesized organic polymer acidic catalysts, HNTs-PSt-PDVB-SO_3H(I) and HNTs-PSt-PDVB-SO_3H(II) were selected to study the reusability for the cellulose dehydration reaction over five cycles. The catalysts were recovered by centrifugation after adding a certain amount of H_2SO_4 used as diluents. After filtration, the residue was dried at 80 ^oC to get powders as catalysts. All reaction conditions were same as the optimized conversion experiments. As shown in Fig. 10a, the yields of HMF maintained at around 26.26% and 31.02% till the fifth run for HNTs-PSt-PDVB-SO_3H(I) and HNTs-PSt-PDVB-SO_3H(II), which were as comparable as that of fresh catalysts, respectively. No significant loss of HMF yield was observed till the fifth run meant that the immobilized functional groups of -SO_3H did not leach largely during the complicated and repeated process. The superior recyclability of

HNTs-PSt-PDVB-SO_3H(I) and HNTs-PSt-PDVB-SO_3H(II) came from their superior thermal stability of both acidic sites and polymer network, which were very important for their widely practical applications. These results, to some extent, suggested that the heterogeneous catalysts has the potential to be effectively separated and reused for the dehydration reaction.

Fig. 10b and Fig. 10c showed the contact angle for water of HNTs-PSt-PDVB-SO_3H(I) and HNTs-PSt-PDVB-SO_3H(II) used in the fifth run experiment, respectively. We can get the conclusion that the fifth used HNTs-PSt-PDVB-SO_3H(I) and HNTs-PSt-PDVB-SO_3H(II) give the contact angle at 97.58^o and 94.84^o, respectively. These catalysts both showed relatively hydrophobicity after used five turns. The process of catalyst immersed with 1.0 M of H_2SO_4 for 12 hours may lead to more hydrophilic group -SO_3H introduced onto the surface of HNTs-PSt-PDVB-SO_3H(I) and HNTs-PSt-PDVB-SO_3H(II), resulting in the reduce of contact angle for water. Furthermore, the superior recyclability of HNTs-PSt-PDVB-SO_3H(I) and HNTs-PSt-PDVB-SO_3H(II), indicating the group -SO_3H was strongly grafted onto the surface of HNTs-PSt-PDVB(I) and HNTs-PSt-PDVB(II) during our sulfonation process.

Insert Fig. 10 (A) Recyclability of HNTs-PSt-PDVB-SO_3H(I) and HNTs-PSt-PDVB-SO_3H(II) in cellulose-to-HMF conversion. Reaction conditions for HNTs-PSt-PDVB-SO_3H(I): cellulose = 0.1 g, ILs = 2.0 g, catalysts = 0.1 g, T = 110 ^{o}C, t (pre-treatment)=0.5 h, t (reaction)=1 h, for HNTs-PSt-PDVB-SO_3H(II): cellulose = 0.1 g, ILs = 2.0 g, catalysts = 0.05 g, T = 120 ^{o}C, t (pre-treatment)=0.5 h, t (reaction)=2 h. (B) Contact angle for water of HNTs-PSt-PDVB-SO_3H(I) (b) and HNTs-PSt-PDVB-SO_3H(II) (c) used in the fifth run experiment.

4. Conclusions

In this work, two ways such as precipitation polymerization and Pickering emulsion polymerization were considered to be effective methods for preparing polymeric acid catalysts, and the natural clay HNTs were also approved to be satisfactory supports for precipitation polymerization and perfect stabilizer for Pickering emulsion polymerization. The catalytic activity and recyclability of as-prepared HNTs-PSt-PDVB-SO_3H(I) and HNTs-PSt-PDVB-SO_3H(II) were successfully evaluated in the process of cellulose-to-HMF conversion, and obtained yield of HMF at 28.22% for HNTs-PSt-PDVB-SO_3H(I) and 32.86% for HNTs-PSt-PDVB-SO_3H(II) at the

optimized conditions. This work was the continue efforts for making stable polymeric solid acid, and the results from this work could be valuable for future research towards development of new reactors, especially their wide application for biomass and bioenergy.

References

1 L.L. Zhou, R.J.Liang, Z.W.Ma, T.H.Wu, Y. Wu, Bioresour. Technol. 2013, 129, 450-455.

2 A.A. Rosatella, S.P. Simeonov, Frade, R.F.M., Afonso, C.A.M., Green Chem. 2011, 13, 754-793.

3 E.Z. Małgorzata, B.Ł. Ewa, B.Ł. Rafał, Chem. Rev. 2011, 111, 397-417.

4 F. Guo, Z. Fang, T. Zhou, Bioresour. Technol. 2012, 112, 312-318.

5 O. Yemis, G. Mazza, Bioresour. Technol. 2012, 109, 215-223.

6 Y. Su, H.M. Brown, X.W. Huang, X.D. Zhou, E.A James, Z.C. Zhang, Appl. Catal. A-Gen. 2009, 361, 117-122.

7 F. Jiang, Q.J. Zhu, D. Ma, X.M. Liu, X.W. Han, J. Mol. Catal. A-Chem. 2011, 334, 8-12.

8 S.H. Xiao, B. Liu, Y.M. Wang, Z.F. Fang, Z.H. Zhang, Bioresour. Technol. 2014, 151, 361-366.

9 S. M. Notley, B. Pettersson, L. Wagberg, J. Am. Chem. Soc. 2004, 126, 13930-13931.

10 R. Rinaldi, F. Schüth, Chem. Sus. Chem. 2009, 2, 1096-1107.

11 C. Li, Z.K. Zhao, Adv. Synth. Catal. 2007, 349, 1847-1850.

12 W.H. Peng, Y.Y. Lee, C. Wu, C.-W. Kevin, J. Wu, Mater. Chem. 2012, 22, 23181-23185.

13 F.S. Asghari, H. Yoshida, Ind. Eng. Chem. Res. 2007, 46, 7703-7710.

14 X.M. Zhang, L. Zhang, Q.H. Yang, J. Mater. Chem. A 2014, 2, 5765-5773.

15 G. A. Olah, G. K. S. Prakash, J. Sommer, Science 1979, 206, 13-16.

16 K. Arata, Appl. Catal. A 1996, 146, 3-32.

17 R.J. Gillespie, Acc. Chem. Res. 1968, 1, 202-213.

18 R.J. Gillespie, T.E. Peel, Adv. Phys. Org. Chem. 1972, 9,1-12.

19 S. Julien, E. Chorneta, R.P. Overend, J. Anal. Appl. Pyrol. 1993, 27, 25-43.

20 A.-Y. Hussein, E.B. Hassan, P. Steele, J. Fuel. Chem. Technol. 2013, 41, 214-222.

21 P. Kalita, B. Sathyaseelan, A. Mano, S.M. Javaid Zaidi, M. A. Chari, A. Vinu, Chem. Eur. J. 2010, 16, 2843-2846.

22 J. Gao, J. Liu, S. Bai, P. Wang, H. Zhong, Q. Yang and C. Li, J. Mater. Chem., 2009, 19, 8580-8587.

23 J. Y. Kim, J. C. Park, H. Kang, H. Song and K. H. Park, Chem. Commun., 2010, 46, 439-446.

24 H. Li, Q.Y. Zhang, X.F. Liu, F. Chang, Y.P. Zhang, W. Xue, S. Yang, Bioresour. Technol. 2013, 144, 21-27.

25 K. Li , H.H. Stöver, J. Polym. Sci. Part A: Polym. Chem. 1993, 31, 3257-3263.

26 W.H. Li , H.H Stöver . J. Polym. Sci. Part A: Polym. Chem. 1999, 37, 2899-907.

27 J. Downey, R.S. Frank , W.H. Li, H.H. Stöver, Macromolecules 1999, 32, 2838-2844.

28 Y. Chen, L.Y. Tong, D.Y. Zhang, W.T. Yang, J.P. Deng, Ind. Eng. Chem. Res. 2012, 51, 15610-15617.

29 H.O. Zhou, T.J. Shi, X. Zhou. Appl. Surf. Sci. 2013, 266, 33-38.

30 Y.J. Jiang, X.L. Liu, Y.F. Chen, L.Y. Zhou, Y. He, L. Ma, J. Gao, Bioresour. Technol. 2014, 153, 278-283.

31 S.A.F. Bon, P.J. Colver, Langmuir 2007, 23, 8316-8322.

32 N. Wen, Q. Tang, M. Chen, L. Wu, J. Colloid Interf. Sci. 2008, 320, 152-158.

33 P. Pieranski, Phys. Rev. Lett., 1980, 45, 569-570.

34 H. Lehle, E. Noruzifar, M. Oettel, Eur. Phys. J. E: Soft Matter Biol. Phys., 2008, 26, 151-160.

35 C.H. Zhou, Appl. Clay Sci. 2011, 53, 87-96.

36 S.R. Levis, P.B. Deasy, Int. J. Pharmaceut. 2002, 243, 125-134.

37 X.M. Sun, Y. Zhang, H.B. Shen, N.Q. Jia, Electrochim. Acta. 2010, 56, 700-705.

38 Y.L. Zhang, J.M. Pan, M.Y. Gan, H.X. Ou, Y.S. Yan, W.D. Shi, L.B. Yu, RSC ADV. 2014, 4, 11664-11672.

39 Y. Zhang, R.J. Liu, Y.L. Hu, G.K. Li. Anal. Chem. 2009, 81, 967-976.

40 A. Dutta, D. Gupta, A. K. Patra, B. Saha, .A.Bhaumik, Chem. Sus. Chem. 2014, 7, 925-933.

41 M. Zhao, P. Liu, J. Therm. Anal. Cal. 2008, 94, 103-107.

42 J. Scaranto, A.P. Charmet, S. Giorgianni, J. Phys. Chem. C. 2008, 112, 9443-9450.

43 M. Selvaraj, P.K. Sinha, A. Pandurangan. Micropor. Mesopor. Mater. 2004, 70, 81-91.

44 C.N.R. Rao, Angew. Chem. Int. Edit. 1965, 77, 391-398.

45 D. Liu, P. Yuan, H.M. Liu, J.G. Cai , Z.H. Qin, D.Y. Tan, Q. Zhou, H.P. He, J.X. Zhu, Appl. Clay Sci. 2011, 52, 358-363.

46 R.C. Ravindra, Y.S. Bhat, G. Nagendrappa, B.S. Jai Prakash, Catal. Today 2009, 141, 157-160.

47 D. Liu, P. Yuan, H.M. Liu, J.G. Cai, D.Y. Tan, H.P. He ,J.X. Zhu, T.H. Chen. Appl. Clay Sci. 2013, 80,407-412.

48 F. J. Liu, X.-J. Meng, Y. L. Zhang, L. M. Ren, F. Nawaz, F.-S. Xiao, J. Catal. 2010, 271, 52-58.

49 N. Bother, F. Descher, J. Klein, H. Widdecke, Polymer 1979, 20, 850-854.

50 A.I. Torres, P. Daoutidis, M. Tsapatsis, Energy Environ. Sci. 2010, 3, 1560-1572.

51 J.N. Chheda, Y. Roman-Leshkov, J.A. Dumesic, Green Chem. 2007, 9, 342-350.

52 M. E. Zakrzewska, E. Bogel-Lukasik, R. Bogel-Lukasik, Chem. Rev. 2011, 111, 397-417.

53 Y. Rom┘ n-Leshkov, J. N. Chheda, J. A. Dumesic, Science 2006, 312, 1933-1937.

54 H. B. Zhao, J. E. Holladay, H. Brown, Z. C. Zhang, Science 2007, 316, 1597-1600.

55 P. Lanzafame, D.M. Temi, S. Perathoner, A.N. Spadaro, G. Centi. Catal. Today 2012, 179, 178-184.

56 C. Flora, R. Franck, P. Catherine, C. Amandine, G. Emmanuelle, E. Nadine. Appl. Catal. B-Environ. 2011, 105,171-181.

57 Z.D. Ding, J.C. Shi, J.J. Xiao, W.X. Gu, C.G. Zheng, H.J. Wang. Carbohyd. Polym. 2012, 90, 792-798.

ACKNOWLEDGMENTS

This work was financially supported by the National Natural Science Foundation of China (No. 21107037, No. 21176107, No.21306013), Natural Science Foundation of Jiangsu Province (No. BK2011461, No. BK2011514), National Postdoctoral Science Foundation (No.2013M530240), Postdoctoral Science Foundation funded Project of Jiangsu Province (No. 1202002B) and Programs of Senior Talent Foundation of Jiangsu University (No. 12JDG090).

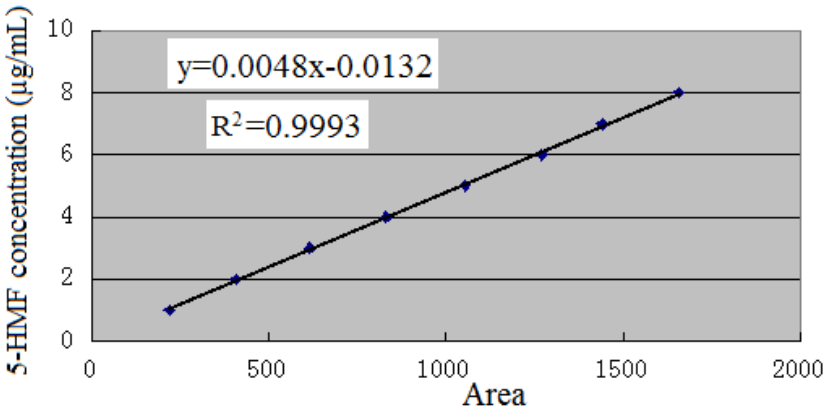

Fig.1 Calibration curve of HMF

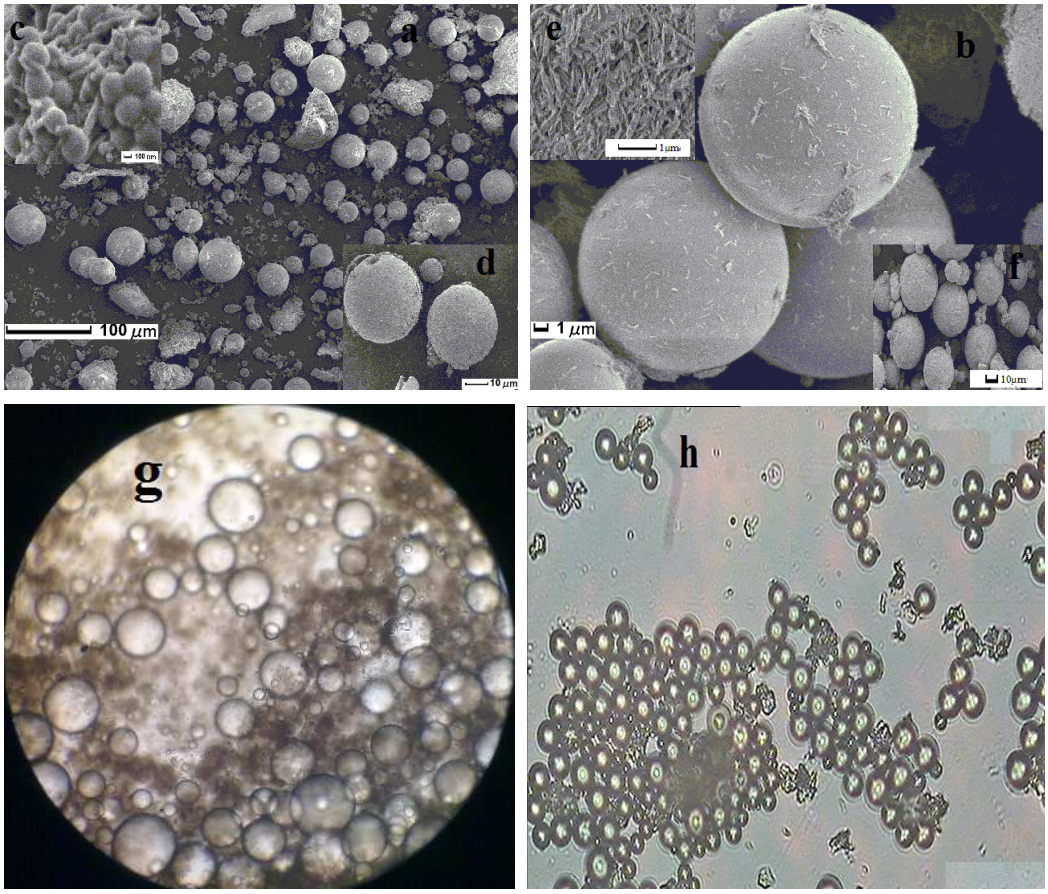

Fig. 2 (A) SEM of the HNTs-PSt-PDVB(I) (a、c), HNTs-PSt-PDVB(II) (b、e、h) and HNTs-PSt-PDVB-SO_3H(I) (d), HNTs-PSt-PDVB-SO_3H(II) (f). (B) Optical micrographs of Pickering emulsion polymerizations (g) and final dried solid catalyst of HNTs-PSt-PDVB-SO_3H(II) (h).

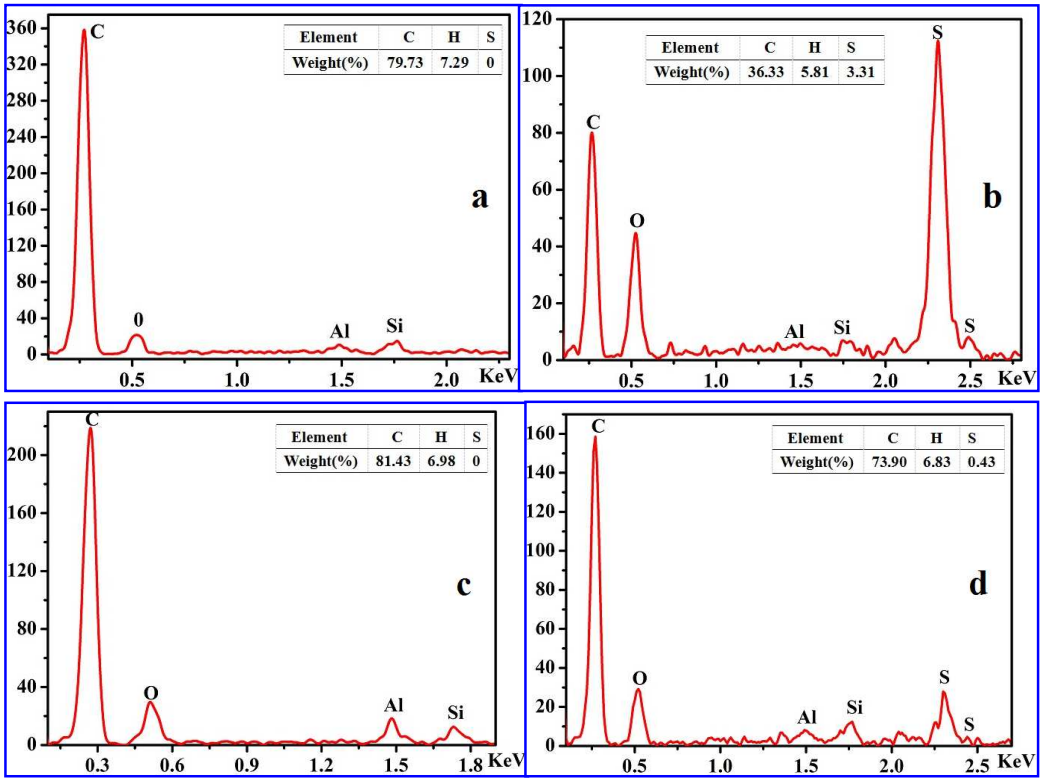

Fig. 3 Energy Dispersive Spectrometer (EDS) and element analysis of the HNTs-PSt-PDVB(I) (a), HNTs-PSt-PDVB-SO_3H(I) (b) and HNTs-PSt-PDVB(II) (c), HNTs-PSt-PDVB-SO_3H(II) (d).

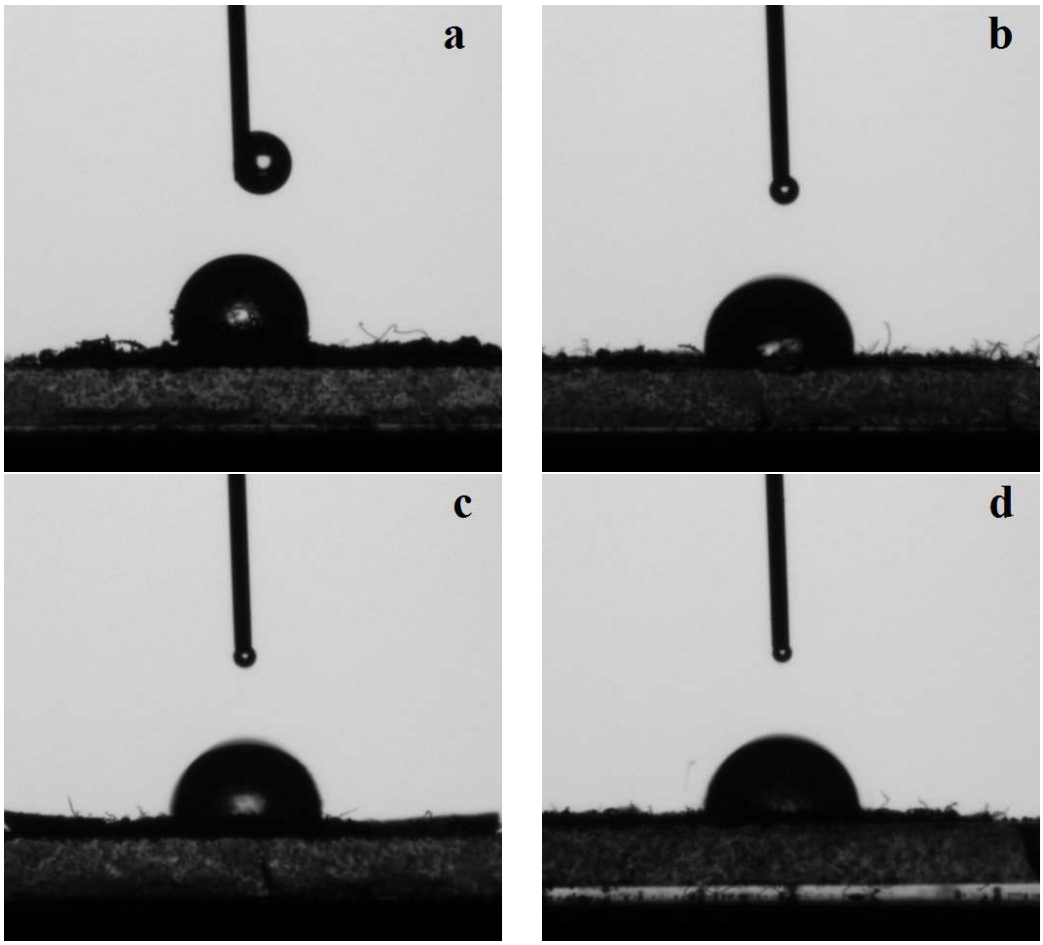

Fig. 4 Contact angle for water of HNTs-PSt-PDVB(I) (a), HNTs-PSt-PDVB-SO_3H(I) (b) and HNTs-PSt-PDVB(II) (c), HNTs-PSt-PDVB-SO_3H(II) (d).

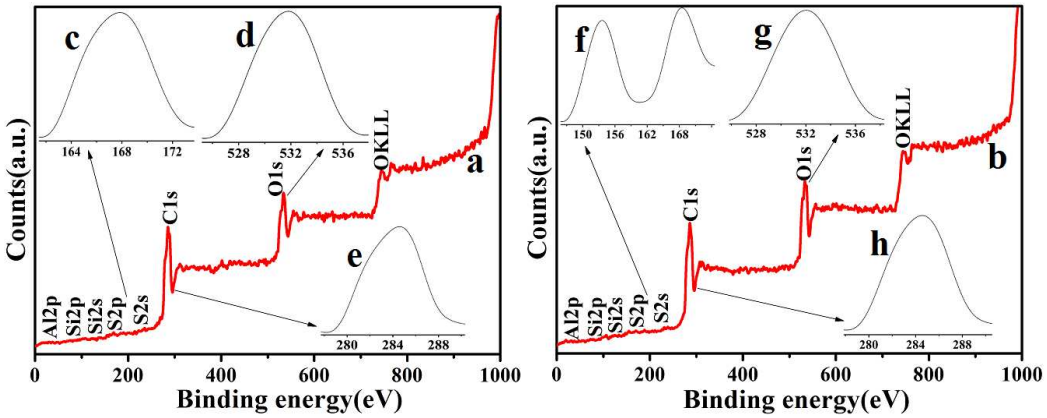

Fig. 5 X-ray photoelectron spectroscopy (XPS) of the HNTs-PSt-PDVB-SO_3H(I) (a) and HNTs-PSt-PDVB-SO_3H(II) (b).

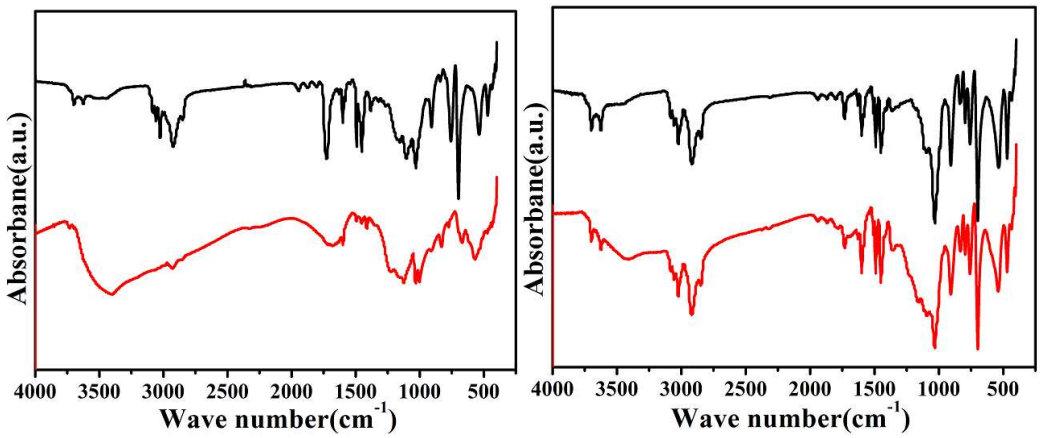

Fig. 6 FT-IR spectra of HNTs-PSt-PDVB(I) (a), HNTs-PSt-PDVB-SO_3H(I) (b) and HNTs-PSt-PDVB(II) (c), HNTs-PSt-PDVB-SO_3H(II) (d).

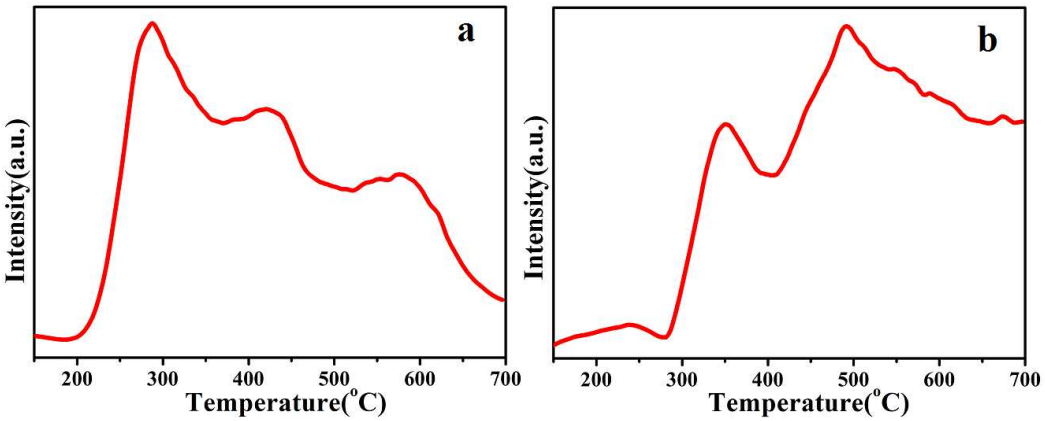

Fig. 7 Temperature programmed desorption (NH_3-TPD) of the HNTs-PSt-PDVB-SO_3H(I) (a) and HNTs-PSt-PDVB-SO_3H(II) (b).

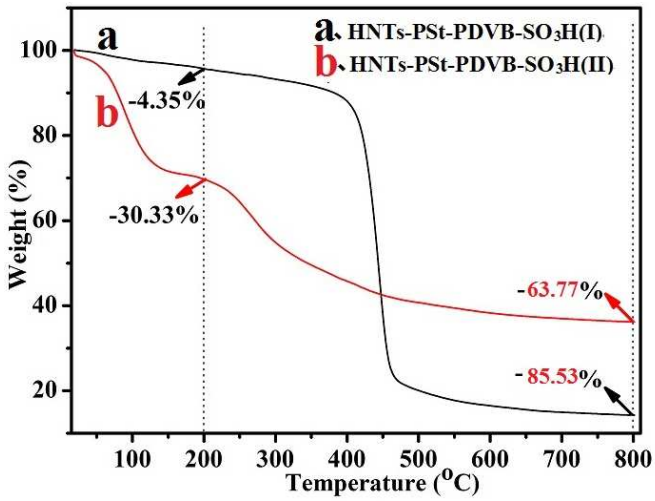

Fig. 8 TG curves of (a) HNTs-PSt-PDVB-SO_3H(I) and (b) HNTs-PSt-PDVB-SO_3H(II).

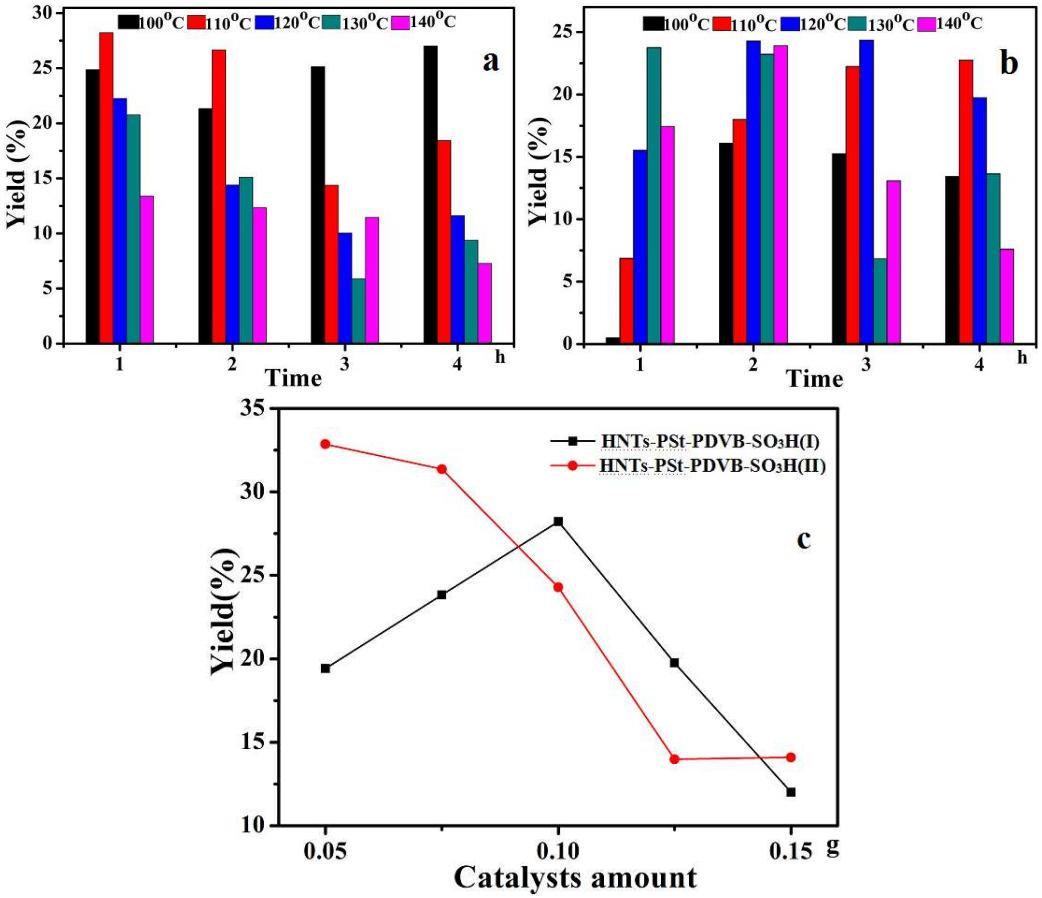

Fig.9 (A) Effect of time and temperature on the yield of cellulose to HMF for HNTs-PSt-PDVB-SO_3H(I) (a) and HNTs-PSt-PDVB-SO_3H(II) (b). (B) Effect of catalyst amount (c).

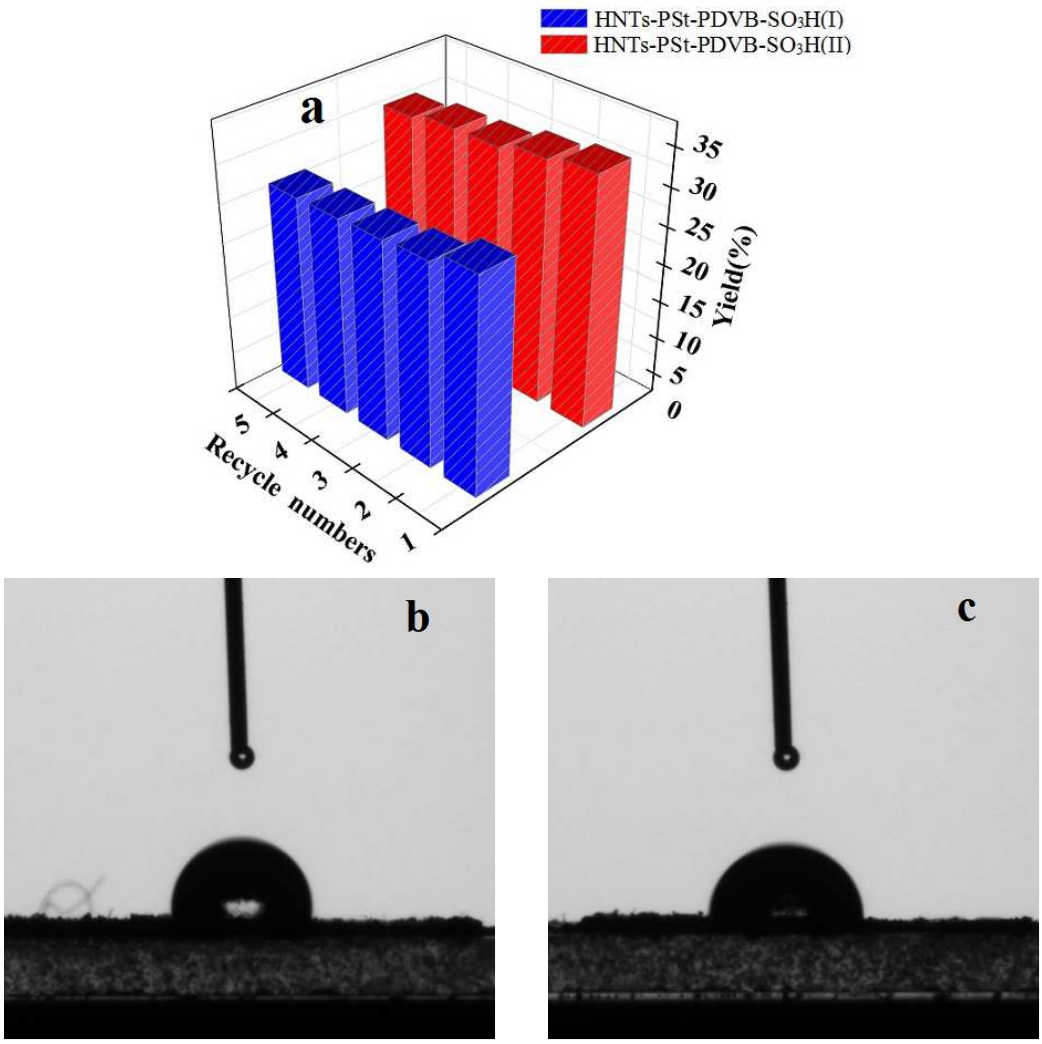

Fig. 10 (A) Recyclability of HNTs-PSt-PDVB-SO_3H(I) and HNTs-PSt-PDVB-SO_3H(II) in cellulose-to-HMF conversion. Reaction conditions for HNTs-PSt-PDVB-SO_3H(I): cellulose = 0.1 g, ILs = 2.0 g, catalysts = 0.1 g, T = 110 ^oC, t (pre-treatment)=0.5 h, t (reaction)=2 h, for HNTs-PSt-PDVB-SO_3H(II): cellulose = 0.1 g, ILs = 2.0 g, catalysts = 0.05 g, T = 120 ^oC, t (pre-treatment)=0.5 h, t (reaction)=2 h. (B) Contact angle for water of HNTs-PSt-PDVB-SO_3H(I) (b) and HNTs-PSt-PDVB-SO_3H(II) (c) used in the fifth run experiment.

Catalyst	HNTs-PSt-PDVB-SO_3H(I)				HNTs-PSt-PDVB-SO_3H(II)			
	250 ^oC	420 ^oC	560 ^oC	Total	250 ^oC	350 ^oC	530 ^oC	Total
Acid strength ($\mu mol\ g^{-1}$)	72	152	88	312	16	36	185	237
Yield (%)	28.22(1.0 h, 110 ^oC and 0.1 g of catalyst)				32.86(2.0 h, 120 ^oC and 0.05 g of catalyst)			
Contact angle	101.29^o				85.14^o			

Table. 1 Acid strength, contact angle and highest yield of HMF for the two catalysts.